Rotenone Model of Parkinson's Disease: Multiple Brain Mitochondria Dysfunctions after Short-term Systemic Rotenone Intoxication

Alexander Panov[1], Sergey Dikalov[2], Natalia Shalbuyeva[3], Georgia Taylor[3], Todd Sherer[3], and J. Timothy Greenamyre[3] Carolinas Neuromuscular/ALS-MDA Center[1], Carolinas Medical Center, Charlotte, NC 28203; Department of Cardiology[2], Center for Neurodegenerative Disease[3], Emory University, Atlanta, GA, 30322

Address correspondence to: Alexander V. Panov, Carolinas Neuromuscular/ALS-MDA Center[1], Carolinas Medical Center, 1000 Blythe Blvd, Charlotte, North Carolina 28203, Tel: 704 355-5902; Fax: 704 446-6255; e-mail: alexander.panov@carolinashealthcare.org

Chronic infusion of rotenone (Rot) to Lewis rats reproduces many features of Parkinson's disease. Rot (3 mg/kg/day) was infused s.c. to male Lewis rats for six days using Alzet minipumps. Control rats received the vehicle only. Presence of 0.1% BSA during the isolation procedure completely removed rotenone bound to the mitochondria. Therefore all functional changes were aftereffects of rotenone toxicity *in vivo*. In Rot rat brain mitochondria (Rot-RBM) there was a 30-40% inhibition of respiration in State 3 and State-3U with Complex I (Co-I) substrates and succinate. Rot did not affect the State-4 $\Delta\Psi$ of RBM and rat liver mitochondria (RLM). However, Rot-RBM required two times less Ca^{2+} to initiate permeability transition (mPT). There was a two-fold increase in $O_2^{\cdot-}$ or H_2O_2 generation in Rot-RBM oxidizing glutamate. Rot infusion affected RLM little. Our results show that in RBM the major site of ROS generation with glutamate or succinate is Co-I. We also found that Co-II generates substantial amounts of ROS that increased two-fold in the Rot-RBM. Our data suggest that the primary mechanism of Rot toxic effect on RBM consists in a significant increase of $O_2^{\cdot-}$ generation that causes damage to Co-I and Co-II, presumably at the level of 4Fe-4S clusters. Decreased respiratory activity diminishes resistance of RBM to Ca^{2+} and thus increases probability of mPT and apoptotic cell death. We suggest that the damage to Co-I and Co-II shifts $O_2^{\cdot-}$ generation from the CoQ_{10} sites to more proximal sites, such as flavines, and makes it independent of the RBM functional state.

Currently, it is widely accepted that mitochondrial dysfunctions play an important role in pathogenesis of neurodegenerative diseases (NDD), such as Parkinson's disease (PD) (1,2), Huntington's disease (3), Amyotrophic Lateral Sclerosis (4), Friedrich's ataxia (5), and others. Various aspects of mitochondrial participation in neurodegeneration have been discussed in numerous recent reviews and papers (2, 6-16). A large progress towards understanding the mechanisms of mitochondrial involvement in neurodegeneration occurred when genetic and toxic animal models of neurodegenerative diseases were developed. Inhibitors of mitochondrial respiratory chain are widely used in toxic models of NDD. The inhibitors of Complex I (MPP^+, rotenone) are used to model Parkinson's disease (1, 16-19), whereas inhibitors of Complex II (3-Nitropropionic acid, malonate) are used to model Huntington's disease (20-22).

Among various animal models of PD, the rotenone model has recently drawn particular attention for two reasons: 1) Unlike other models it reproduces most of the movement disorder symptoms and the histopathological features of PD including Lewy bodies (2, 19) and 2) Rotenone and other pesticides are powerful inhibitors of mitochondrial respiration, and recent epidemiological studies suggest involvement of these toxic compounds in the higher incidence of sporadic Parkinsonism among population of rural areas (23, 24). Since the first publication of Betarbet et al. (1), there have been many published papers describing various aspects of the *in vivo* rotenone model of Parkinsonism in rats (17, 18, 25, 26), and the results have been discussed in several recent reviews (2, 19). Most papers on *in vivo* rotenone intoxication address various aspects of behavioral and morphological signs of parkinsonism (1, 17, 18, 26), but not specific mitochondrial functions, except for nitric oxide generation (25). Therefore, the complete picture of what happens to mitochondria is still absent.

There are three major mitochondrial functions that determine the cell's performance and fate. These are: 1) oxidative phosphorylation that produces ATP for almost all cellular functions, 2) mitochondrial Ca^{2+}-dependent permeability transition (mPT) that may initiate apoptotic or necrotic death of a cell, and 3) generation of reactive oxygen species (ROS) – a byproduct of normal aerobic metabolism. Compelling evidence exist that increased generation of ROS is responsible for the cell's dysfunction and sensitization to death signals. Thus systemic rotenone intoxication may cause damage to each of these major mitochondrial functions or all of them. However, it is unclear how increased ROS production relates to other events leading to the dopaminergic cells death (27). The important issue to be addressed is the time course of pathological events in the systemically poisoned animals.

In this paper we present data on relatively short-term systemic rotenone intoxication (six days). In order to find methods of therapeutic intervention it is important to understand the early primary mechanisms of rotenone

toxicity. We expect that after six days of intoxication the organism will respond to the toxin but various adaptive mechanisms will not yet shadow the primary mechanisms of rotenone toxicity. We show that rotenone intoxication for six days results in multiple mitochondrial dysfunctions including increased ROS generation, inhibition of NAD-dependent substrates oxidation, and, surprisingly, succinate oxidation. Importantly, the inhibition of succinate oxidation was the most consistent fact that we observed both after short-term and long-term (four weeks) rotenone intoxication. Also we show that in rat brain mitochondria (RBM) Complex II also generates ROS at a rate comparable with the rate in the presence of glutamate + malate. Although rotenone intoxication results in a 42% decrease of succinate-supported ROS generation at Complex I associated with the backward electron flow, there was a two-fold increase of ROS generation by Complex II itself, which increased even further (3-4-fold) after four weeks of rotenone intoxication (unpublished data). We suggest that inhibition of electron flow at Complexes I and II results from the damages to 4Fe-4S clusters. As a result, the intraprotein sites of $O_2^{\cdot-}$ generation shift to more proximal sites, presumably flavines, and thus generation of ROS in Rot-RBM becomes independent of the mitochondrial metabolic state. These changes lead to a higher probability of permeability transition of the brain mitochondria when challenged with Ca^{2+}, and thus excitotoxic cell death. Unlike RBM, rotenone affected RLM little. Thus a complex interaction of several mitochondrial dysfunctions in the brain during systemic rotenone dysfunction is responsible for selective loss of neurons in this model of PD.

EXPERIMENTAL PROCEDURES

Animals - Male Lewis rats weighing 300-350 g were used in this study. All animal use complied with National Institutes of Health guidelines and was approved by the Emory University Institutional Animal Care and Use Committee.

Subcutaneous implantation of osmotic pumps. Alzet osmotic minipumps (Alzet Corporation, Palo Alto, CA) were filled with rotenone (Sigma, St. Louis, MO) dissolved in equal volumes of dimethyl sulfoxide (DMSO) and polyethylene glycol (PEG-300, Sigma) or solvent alone as described in (17). Ketamine (75 mg/kg) and xylazine (10 mg/kg) were injected intramuscularly for anesthetic. Alzet osmotic minipumps were implanted under the skin on the back of each animal (17). Control rats received DMSO: PEG (1:1) only. Treated rats received 3.0 mg/kg/ day rotenone (based on the weight at the time of surgery). The animals were sacrificed on the 6^{th} day after surgery.

Isolation of rat liver and brain mitochondria - Both liver and brain mitochondria were isolated in medium containing the following: (in mM) 225 mannitol, 75 sucrose, 20 MOPS (pH 7.2), 1 EGTA, and 0.1% BSA. Liver mitochondria (RLM) were isolated by conventional differential centrifugation with a final spin at 8600 g (28). Brain mitochondria were isolated from the pooled forebrains of three rats. We used the modified method of Sims (29) to isolate and purify brain mitochondria (RBM) in a Percoll gradient. The modifications were as follows: brain tissue was homogenized with 15 strokes of a loose pestle in a Dounce homogenizer, and 5 ml volumes per tube of 15%, 23% and 40% (v/v) of Percoll solutions were used to purify the brain mitochondria. After the final sedimentation of mitochondria at 8600 g, the mitochondria were suspended in 250 mM sucrose and 10 mM MOPS (pH 7.2). Mitochondrial protein was determined using the Pierce Coomassie Protein Assay Reagent Kit.

Preparation of the submitochondrial particle -. The inverted nonphosphorylating submitochondrial particles (SMP) were prepared according to (30). Fresh RLM or RBM mitochondria were suspended in 0.25 M sucrose with 2 mM EDTA to contain about 20-30 mg/ml. 0.5 ml of the suspension was saturated with N_2, placed into a beaker filled with a mixture of ice, water and KCl for effective cooling, and subjected to sonic oscillations (5 times for 5 seconds). The sonicated mitochondria were diluted with a double volume of 0.25 mM sucrose buffered with 10 mM MOPS, and centrifuged in a Beckman ultracentrifuge at 16,000g for 10 minutes. The supernatant was centrifuged at 150,000 g (rotor SW41) for 45 minutes. The sediment of SMP was collected and homogenized in a small glass homogenizer in a volume of 0.25 M sucrose to give final concentration of SMP of 10-20 mg/ml. The usual recovery of the protein as SMP was about 20-30% of the original concentration of the mitochondria.

Simultaneous registration of mitochondrial respiration and membrane potential. - Respiratory activities of the mitochondria were measured using a custom made plastic minichamber of 765 µl volume equipped with a standard YSI (Yellow Spring Instrument Co., Inc.) oxygen minielectrode connected to a YSI Model 5300 Biological Oxygen Monitor, a custom made Tetraphenylphosphonium (TPP^+) - sensitive minielectrode, and a KCl bridge to a Ag/AgCl reference electrode connected to a pH meter. All instruments were connected to a Keep & Zonnen paper chart recorder and the data acquisition system. To obtain maximum oxidative phosphorylation activity (see 31) the following incubation medium was used (Medium A): (in mM) 125 KCl, 10 MOPS, pH 7.2, 2 $MgCl_2$, 2 KH_2PO_4, 10 NaCl, 1 EGTA, 0.7 $CaCl_2$. At Ca^{2+}/EGTA ratio of 0.7 the free [Ca^{2+}] is close to 1 µM as determined with Fura-2 method (31). The substrate concentrations were as follows: (in mM) 5 succinate without rotenone, 20 glutamate + 2 malate, 5 pyruvate + 2 malate, 10 α-ketoglutarate + 2 malate. Oxidative phosphorylation (State 3) was initiated by addition of 150 µM ADP. The uncoupled respiration (State 3U) was stimulated by titration with CCCP (0.05 µM aliquots) until maximum rate of oxygen consumption was obtained.

Membrane potential was measured with a tetraphenylphosphonium (TPP^+) -sensitive electrode as described in (28, 32). Because the volume of the matrix space and binding constants for TPP^+ in brain mitochondria are unknown, the calculated $\Delta\Psi$ values were approximate.

Registration of permeability transition and estimation of calcium retention capacity (CRC). - We have introduced a quantitative parameter CRC that allows a meaningful comparison of the sensitivity to Ca^{2+} of mitochondria from different organs and species (33). CRC is the amount of calcium that can be accumulated and retained by mitochondria until the Permeability Transition occurs (mPT). It is expressed as nanomol of Ca^{2+} per mg of mitochondrial protein. For our work we used two different methods to estimate CRC and register permeability transition: 1) Potentiometric measurements of pH changes of the incubation medium during Ca^{2+} accumulation and release by the mitochondria as described in (33), and 2) Depolarization of the mitochondria using a TPP^+-sensitive electrode as described elsewhere (33). The pH measurements were performed using Corning pH meter model 440 equipped with a mono pH microelectrode from Lazar Co., and Ag/AgCl reference electrode connected to the incubation chamber by a KCl bridge.

The mitochondrial CRC values were estimated in medium (Medium B) containing: (in mM) 125 KCl, 10 NaCl, 0.5 $MgCl_2$, 3 glycyl-glycin, pH 7.2, 1 KH_2PO_4, and 20 glutamate + 5 malate as substrates for brain and liver mitochondria. Mitochondrial protein was 0.5 mg/ml. Measurements were done in a final volume of 1.0 ml. Ca^{2+} was added to mitochondria in 5 µl aliquots of 5, 10, or 20 mM stock solutions of $CaCl_2$ of very high purity – 99.99% (Sigma). *Measurements of hydrogen peroxide generation.* - H_2O_2 was measured using the Amplex Red (Molecular Probes). In the presence of horseradish peroxidase (HRP) there is a reaction: Amplex Red + H_2O_2 ⏲ Resorufin + O_2. Resorufin is a stable and highly fluorescent compound whose wavelength spectra excitation/emission are 570/585 nm. The fluorescence of resorufin was determined in 1 ml incubations in Medium A, 0.2 mg/ml mitochondrial protein, 5 µM Amplex Red and 3 units of HRP. Calibration was made using standard solutions of H_2O_2 (Fluka) and resorufin (Sigma). Fluorimetric measurements were made using fluorometer from C&L Company, Middletown, Pennsylvania. Resorufin was measured using an excitation filter of 570 nm, and the emission filter was of 585 nm. The stock solutions of the mitochondrial inhibitors used for inhibitor analysis of H_2O_2 generation sites were made in ethanol.

Measurements of $O_2^{\cdot}$- release by mitochondria. - The cyclic hydroxylamine PPH (Alexis Biochemicals, San Diego, CA) was used for quantitative measurements of $O_2^{\cdot}$- release by mitochondria. PPH allows extracellular and extramitochondrial detection of $O_2^{\cdot}$- (34). It reacts with $O_2^{\cdot}$- producing stable PP-nitroxide detected with ESR spectroscopy (Figure 1, insert). Briefly, 10 mM PPH was dissolved in deoxygenated media with 50 µM deferoxamine. Mitochondria preparations and PPH stock solutions were kept on ice. 50 µg protein mixed with 1 mM PPH and mitochondrial substrates in 100 µl Medium A. Detection of $O_2^{\cdot-}$ radical was confirmed by inhibition of ESR signal with 50 U/ml superoxide dismutase (Figure 1). Accumulation of PP-nitroxide was measured using a Bruker EMX ESR spectrometer and a super-high Q microwave cavity. The concentration of PP-nitroxide was determined by calibration with standard concentrations of 3-carboxyproxyl nitroxide (Alexis Biochemicals, San Diego, CA). Superoxide production was detected by following the low-field peak of the nitroxide ESR spectra (Figure 1, insert) using time scans with the following ESR settings: microwave frequency 9.78 GHz, modulation amplitude 2 G, microwave power 10 dB, conversion time 1.3 sec, and time constant 5.2 sec.

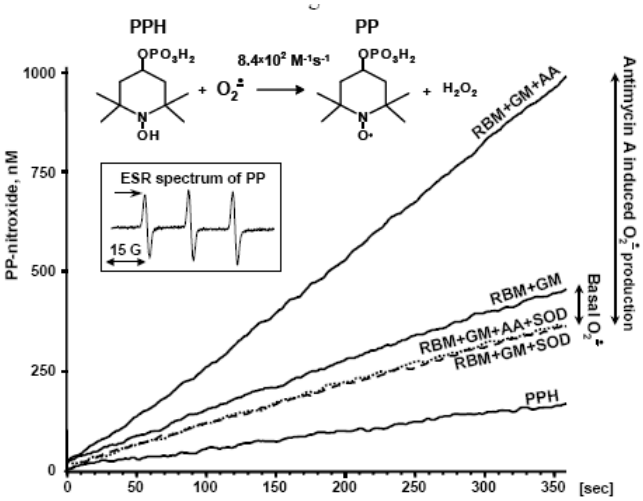

Figure 1. Measurements of $O_2^{\cdot}$- release by mitochondria using ESR and spin probe PPH.

PPH reacts with $O_2^{\cdot}$- producing stable PP-nitroxide detected with ESR spectroscopy (insert). Superoxide radicals were measured by SOD-inhibited ESR signal of PP-nitroxide in the sample containing mitochondria, substrate and PPH as described in the Method section.

Data acquisition. Data acquisition was performed using hardware and software from C & L Company, Middletown, Pennsylvania. *Chemicals* - Chemicals were of highest purity available. All solutions were made using glass bidistilled water.

Statistics - Data are presented as mean ± standard error. For comparison of two groups, a two-tailed *t*-test was employed using Excel software. Statistical significance was assumed when $p < 0.05$.

RESULTS

Mitochondrial yields. Using our standard procedure for isolation of brain and liver mitochondria with a final sedimentation at 8,600 g, we have found that the yield of brain mitochondria (normalized per 1 gram of wet tissue) was on average 20% higher for rotenone-treated animals (1.74 ± 0.14 mg RBM/mg wet tissue) as compared to the sham operated rats (1.44 ± 0.1 mg RBM/mg wet tissue). There was no change in mitochondrial yields from the livers of rotenone rats. Interestingly, Koopman et al. (35) recently reported that in cells chronically treated with rotenone there is a significant increase in mitochondrial length and branching without changing the number of mitochondria per cell. Evidently, the increased yield of RBM from Rot-rats was not associated with glia because at this early stage of rotenone intoxication there was no significant increase in the number of glial cells in the brain (1).

Effects of systemic rotenone infusion on respiratory activities and membrane potential of the rat liver and brain mitochondria. Mitochondrial oxidative phosphorylation is evaluated by measuring the respiratory activity in different metabolic states. When mitochondria oxidize a substrate but do not perform useful work such as ATP generation or cation transport, the membrane potential is at maximum and the rate of oxygen consumption is controlled by the intrinsic proton conductivity of the inner membrane (reviewed in 36). This is metabolic State 4. When ADP is added to the incubation medium, the mitochondria begin to convert ADP to ATP. As a result of this energy-consuming process, membrane potential drops and the respiratory rate accelerates several fold. This is the metabolic State 3. The ratio of the respiratory rate in State 3 to that in State 4 (V_{St3}/V_{St4}) is known as the Respiratory Control Ratio (RCR) that reflects the ATP-producing capacity of the mitochondria and their quality. When mitochondrial membrane potential is collapsed by addition of a protonophore (in our case CCCP) respiratory rate becomes maximal provided that transport of a substrate is not rate limiting. This is metabolic Sate 3U (uncoupled).

Table I shows that after six days of rotenone infusion there is a significant inhibition of the brain mitochondria (Rot-RBM) respiration with all substrates in metabolic states 3 and 3U as compared to control rats receiving DMSO + PEG only. We did not found any difference between the control untreated rats and the rats exposed for six days to DMSO + PEG. The State 4 respiratory rates with Rot-RBM were also inhibited but not significantly. Remarkably, oxidation of succinate in State 3 and 3U, which is a Complex II substrate, was inhibited to the same degree (~ 40%) as oxidation of Complex I substrates pyruvate and α-ketoglutarate, and more than glutamate (Table I). Inhibition of respiration with these substrates was not associated with diminished activity of Complex IV because with 5 mM ascorbate + 0.3 mM TMPD the rates of oxygen consumption in State 3U were (in nanogram atom O/min/mg protein) 2368 ± 180 for control RBM and 1988 ± 236 for Rot-RBM. Interestingly, after 4 weeks of rotenone intoxication the rate of ascorbate + TMPD oxidation in State 3U was inhibited by 62% (our unpublished data).

In Rot-RLM oxidation of succinate was practically unaffected. However, there was a 50% inhibition of the State 3 glutamate oxidation. Other substrates of Complex I, pyruvate and α-ketoglutarate, were also inhibited. However, the State 3 and State 3U respiratory rates with these substrates were very slow as compared with glutamate. Evidently, livers of Lewis rats do not utilize glucose as a source of energy for mitochondria.

Because of a more profound inhibition of the State 3 oxidation of the substrates as compared to the State 4 respiration, there was a significant decline in the respiratory control ratios in RBM and RLM with all substrates as shown in Figures 2A and 2B, with exception of RLM oxidizing α-ketoglutarate + malate (see Figure 2B).

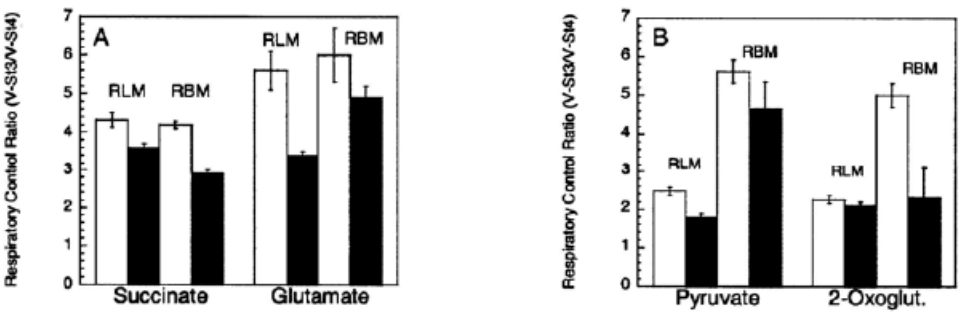

Figure 2. Effect of the *in vivo* rotenone treatment on respiratory control ratios of rat brain and liver mitochondria oxidizing different substrates. Incubation conditions are described in Methods. Lighter columns represent control animals, darker columns – rotenone-treated rats.

The first question that arises regarding the observed inhibitions of the Complex I substrates oxidation in rat brain and liver mitochondria of the rotenone-treated rats (Table I) is whether the inhibitions were associated with a damage of Complex I or by rotenone that may remain bound to the mitochondrial Complex I. In order to answer this question we isolated normal rat brain mitochondria and added *in vitro* 400 nm/mg protein rotenone. This concentration of rotenone inhibits the State 3 oxidation of glutamate + malate by 80-90% (1). The rotenone-loaded and control RBM were then washed twice in 30 ml of the isolation medium (see Methods) that contained 0.1% defatted BSA. The resulting mitochondrial sediments were resuspended and the State 3 and State 3U respiratory rates with glutamate were compared. We found that washing of the rotenone-loaded RBM with the BSA-containing medium completely removed rotenone from the mitochondria (data not shown). Therefore, we suggest that the rotenone was removed from the mitochondria isolated from rotenone treated animals because both RLM and RBM were isolated in the presence of 0.1% BSA. Thus inhibitions of the Complex I substrates oxidation observed in the Rot-RBM and Rot-RLM were indeed associated with a damage of Complex I. A 40% inhibition of the State 3 and State 3U succinate oxidation in RBM also speaks in favor of damage of Complex II because rotenone *in vitro* has no direct effect on succinate oxidation.

In line with insignificant inhibitions of the State 4 respiration in the Rot-RBM, rotenone at this stage of intoxication had no effect on the resting membrane potentials in both Rot-RBM and Rot-RLM (data not shown). This suggests that after 6 days of rotenone intoxication the inner mitochondrial membrane was not yet damaged by lipid peroxidation or other mechanisms (such as oxidative damage of transmembrane proteins) that would result in increased proton conductivity of the inner mitochondrial membrane. However, when a functional load was imposed on the mitochondria (such as phosphorylation of ADP) with Rot-RBM, the drop in membrane potential was larger and it took more time to phosphorylate the same amount of ADP as compared to the control RBM oxidizing glutamate + malate or succinate (not shown). Thus Rot-RBM have diminished ability to maintain energization during increased energy demands due to diminished activities of Co-I and Co-II. This assumption was further studied using Ca^{2+} consumption as an energy dependent function.

Effects of systemic rotenone infusion on permeability transition and the calcium retention capacity (CRC) of RBM and RLM. The amount of calcium phosphate salts (CaPi) that mitochondria can sequester and retain determines whether mitochondria will undergo mPT or not when a cell is challenged with calcium. The data published in the literature suggest that Ca^{2+}-induced mPT may be responsible for the excitotoxic death of glutamatergic neurons (37). Figure 3A shows CRC for RBM and RLM when the mitochondria were not protected by ADP or Cyclosporin A. Rot-RBM required 50% less Ca^{2+} to open the Permeability Transition Pore (mPTP) than control RBM. ADP (in the presence of oligomycin to prevent phosphorylation of ADP) significantly increases CRC, particularly in brain mitochondria (33). This is a more physiological situation because ADP is always present in the cell (38). Figure 3B shows that although in the presence of ADP + oligomycin CRC increased several folds, in Rot-RBM CRC was 27% lower as compared to control RBM. However, when the mitochondria were protected by Cyclosporin A – a specific inhibitor of the mitochondrial permeability transition pore (mPTP) opening (Fig. 3C), the CRC of Rot-RBM was the same as that of control RBM. We used CsA together with ADP because ADP is always present in the cells, and ADP substantially increases CsA binding to mitochondria (39). We have also shown recently that the protective effect of CsA alone is small with brain mitochondria (33). Thus rotenone affects only the energy-dependent CaPi sequestration process without direct influence on mPTP.

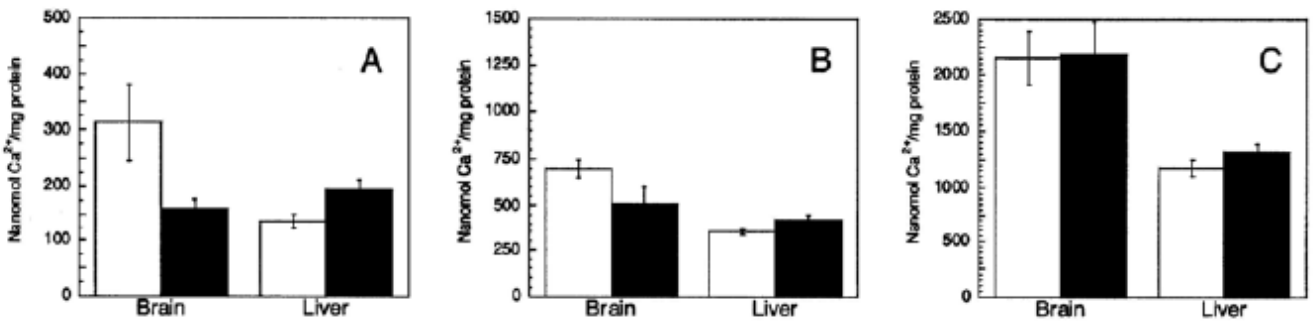

Figure 3. Calcium retention capacity of rat brain and liver mitochondria from control and rotenone-treated rats. Incubation conditions: Medium B (see Methods), glutamate 20 mM, malate 2 mM, mitochondria 0.5 mg, volume 1 ml. Ca^{2+} additions in A 5 µl 10 mM, in 3B and 3C 10 µl of 10 mM stock solution with 1 minute intervals. **A**. Medium with

substrates only – Unprotected mitochondria; **B**. 50 μM ADP + 1 μg oligomycin A; **C**. 0.5 μM Cyclosporin A, 50 μM ADP, 1 μg oligomycin.

Figures 3A, 3B, and 3C show that under all conditions the CRC of RLM was not affected by the systemic rotenone intoxication. There usually was even a slight increase in the resistance of Rot-RLM to calcium loads.

Effects of systemic rotenone infusion on generation of superoxide radical and H_2O_2 by RBM and RLM.

Superoxide radical ($O_2^{\cdot-}$) and H_2O_2 are natural products of mitochondrial aerobic metabolism when electrons spontaneously reduce molecular oxygen (40). Figure 4 compares the rates of $O_2^{\cdot-}$ production by the RBM and RLM. The SOD-inhibitable PP-nitroxide formation reflects the amount of $O_2^{\cdot-}$ released from the mitochondria. Note the protein differences in the experiments. When normalized for 1 mg of protein in the presence of antimycin A and with succinate as a substrate, RBM generate six times more $O_2^{\cdot-}$ than RLM. These data demonstrate a much higher potential for $O_2^{\cdot-}$ production by RBM than RLM. Therefore, there are three factors that make RBM the primary target for rotenone-induced oxidative damage: 1) under the State-4 conditions RBM produce more $O_2^{\cdot-}$ than RLM (Figure 4: 14.2 ± 2.3 vs. 7.7 ± 1.6 pmol/min/mg), 2) mitochondrial dysfunction may lead to a 6-fold higher $O_2^{\cdot-}$ production by RBM than RLM (Figure 4), and 3) RBM have less antioxidant protection than RLM (41).

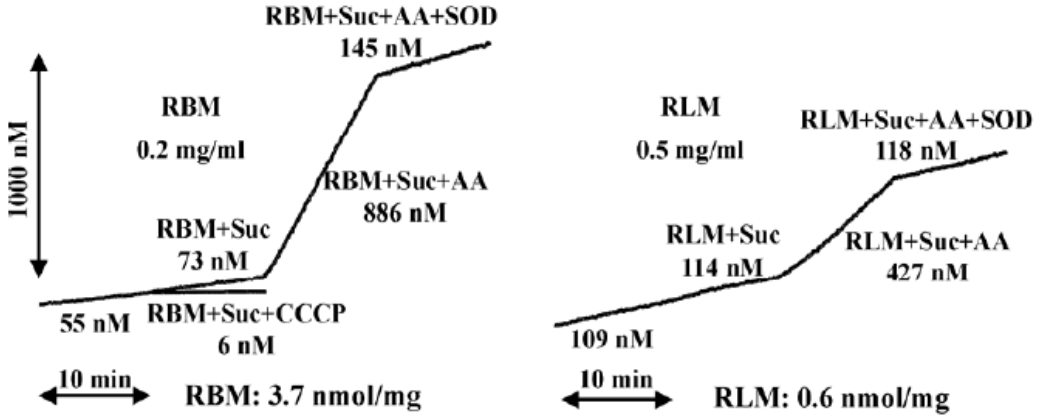

Figure 4. A comparison of superoxide generation by rat brain and rat liver mitochondria.
Incubation conditions: Medium A (see Methods), succinate 5 mM.

Indeed, after six days of systemic rotenone infusion the isolated RBM oxidizing glutamate + malate generated $O_2^{\cdot-}$ at a rate two times faster than RBM from the control animals (Figure 5A, B) (30 ± 3.2 vs 14.2 ± 2.3 pmol/min/mg). At the same time $O_2^{\cdot-}$ production by Rot-RLM oxidizing succinate was not significantly different from the control RLM (Figure 5: 11.0 ± 1.8 vs 7.7 ± 1.6 pmol/min/mg).

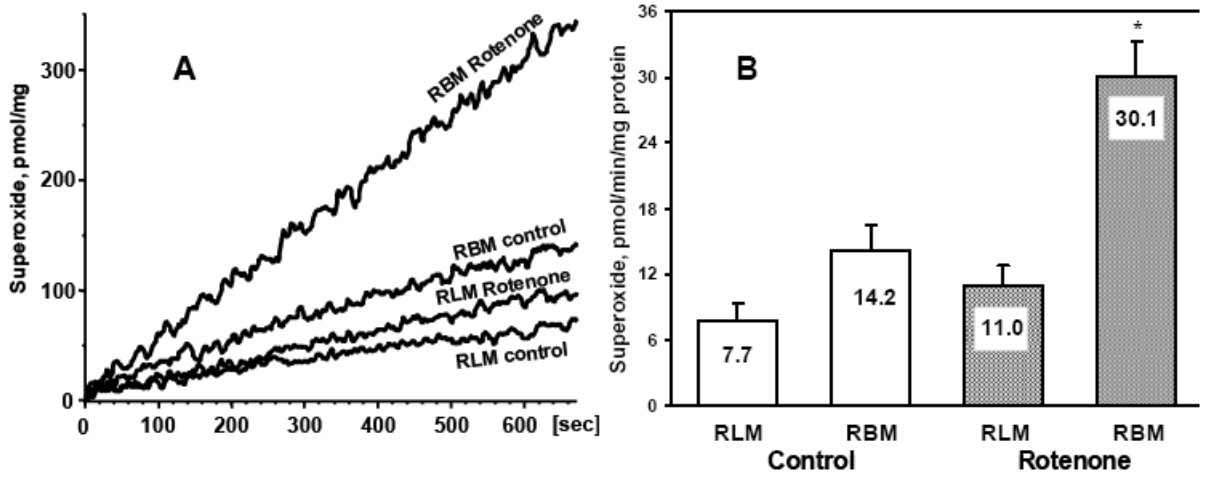

Figure 5. Effect of rotenone infusion on generation of $O_2^{\cdot-}$ by RLM and RBM. Production of $O_2^{\cdot-}$ was measured by SOD-inhibitable oxidation of PPH: (A) kinetics of $O_2^{\cdot-}$ production; (B) amount of detected $O_2^{\cdot-}$.

Interestingly, rotenone added *in vitro* to control RBM oxidizing glutamate + malate leads to a noticeable decrease in $O_2^{\cdot-}$ determined outside the mitochondria (Figure 6A). Experiments conducted with submitochondrial

particles (SMP) from RBM showed that rotenone inhibits the $O_2^{\cdot-}$ release from the mitochondria, but increases its production. Figure 6B shows that rotenone added to SMP caused a four-fold increase in $O_2^{\cdot-}$ generation. Note also that the scale of the Figure 6B is one order larger than that of the 6A. Figure 6C shows that rotenone added *in vitro* to intact RBM doubles the release of H_2O_2. Of interest, the amount of H_2O_2 released was close to that for $O_2^{\cdot-}$ generated by SMP. Addition of SOD1 to the mitochondrial suspension did not further increase generation of H_2O_2 (not shown). Two important conclusions can be drawn from the data presented in figures 6A, B, and C: 1) only a small portion of $O_2^{\cdot-}$ generated by the mitochondria can be determined outside the brain mitochondria, and 2) the release of $O_2^{\cdot-}$ depends on mitochondrial energization. The latter indicates that with the respiratory inhibitors, which are usually used for localization of the sites responsible for ROS generation, the observed $O_2^{\cdot-}$ does not reflect actual $O_2^{\cdot-}$ production by the intact mitochondria. Therefore, generation of H_2O_2 is a more accurate marker of the mitochondrial ROS production under these conditions.

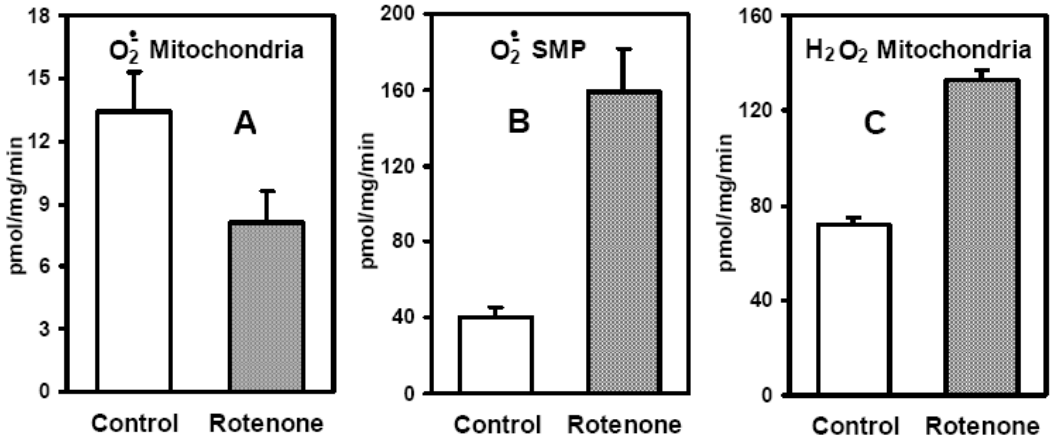

Figure 6. Effect of *in vitro* rotenone (100 pmol/mg) on generation of $O_2^{\cdot-}$ and H_2O_2 by rat brain mitochondria (RBM) and submitochondrial particles (SMP). Incubation conditions as in Table I. Glutamate + malate were used as substrates. (A) Release of $O_2^{\cdot-}$ by intact RBM; (B) Release of $O_2^{\cdot-}$ by SMP from RBM; (C) Release of H_2O_2 by intact RBM. Incubation conditions as described in Methods section. .

After six days of rotenone infusion there was a two-fold increase in H_2O_2 generation with glutamate + malate (Figure 7A) and a 42% decrease with succinate as substrate. The latter occurred possibly due to a 40% inactivation of complex II (Figure 7B). The data presented in figures 7A and 7B - 9A and 9B show that measuring H_2O_2 is probably the best choice to study ROS generation by intact brain mitochondria. Figures 7A and 7B show that RBM from control animals generate 4-5 times more H_2O_2 with succinate as a substrate than with glutamate + malate.

With RLM oxidizing succinate or glutamate + malate there was almost no difference in the rates of H_2O_2 generation (correspondingly 92.1 ± 2 and 80 ± 2 pmol/min/mg protein), which is in stark contrast to production of $O_2^{\cdot-}$ by RBM shown in Figures 7A and 7B. We have also found that with the exception of antimycin A, addition of respiratory inhibitors rotenone, stigmatellin (or myxothiazol), and their combinations to RLM had no effect on the observed rates of H_2O_2 production (not shown). Thus measurements of H_2O_2 cannot be used for analysis of the sites of ROS generation by the liver mitochondria.

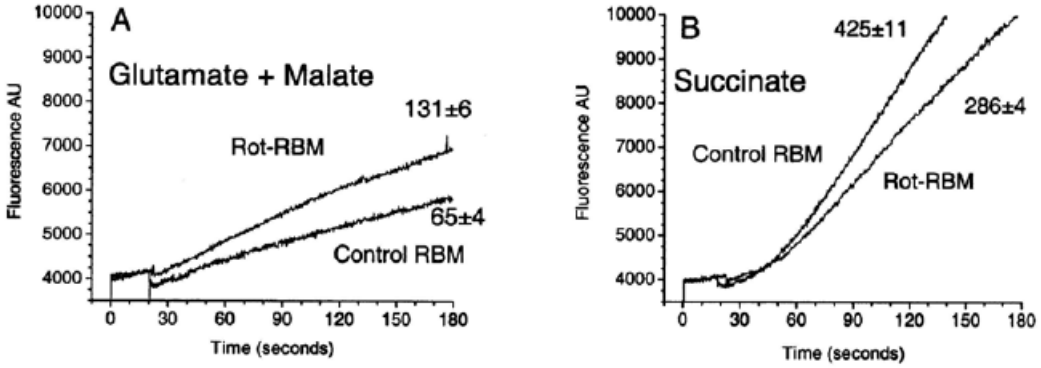

Figure 7. Effects of systemic rotenone intoxication on generation of H_2O_2 by rat brain mitochondria.

Incubation conditions: Medium A, 5 μM Amplex Red, 3 U HRP, 0.2 mg RBM, volume 1 ml.
A. Glutamate 20 mM + malate 2 mM. B. Succinate 5 mM.
The numbers at the traces are the rates of H_2O_2 generation in pmol/min/mg protein.

Inhibitor analysis of the ROS generation sites in RBM from the control and rotenone-treated rats. Figures 8A and 8B show the effects of various respiratory chain inhibitors on generation of H_2O_2 by the control RBM and Rot-RBM oxidizing glutamate + malate. These data show that regardless of the mechanism, inhibition of the electron transport caused a several-fold increase in generation of H_2O_2 by RBM. With glutamate + malate the increase in H_2O_2 upon addition of antimycin A was relatively modest. This might be interpreted as an indication that with Complex I substrates the rate of electrons input from the Complex I limits the rate of $O_2^{\cdot-}$ generation on Complex III in the presence of Antimycin A. It should be mentioned that the rates of H_2O_2 production by RBM oxidizing 5 mM pyruvate + 2 mM malate were very similar to those shown in Figure 7A and 8A for glutamate + malate (pyruvate data are not shown).

The data presented in Figures 8A and 8B show that with glutamate + malate as substrates, the major source of H_2O_2 that reflect generation of $O_2^{\cdot-}$ is Complex I. Figure 8B summarizes quantitatively the results of several experiments with the control RBM and the Rot-RBM. One can see that after six days of rotenone intoxication there was a two-fold increase of ROS generation.

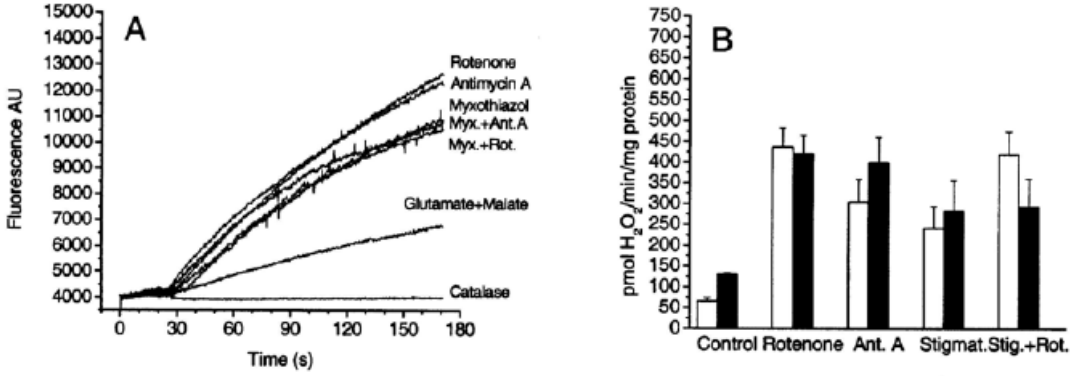

Figure 8 Effects of respiratory inhibitors on H_2O_2 generation by control RBM and Rot-RBM oxidizing glutamate + malate. Incubation conditions as in Fig. 7. A. Responses of control RBM to additions of respiratory inhibitors; B. Generation of H_2O_2 by RBM from the control and rotenone-treated animals. Additions: Catalase (Roche Diagnostics GmbH) 400 μg., Antimycin A 5 μM, Rotenone 5 μM, Myxothiazol 5 μM.

Figures 9A and 9B show the effects of respiratory inhibitors on H_2O_2 generation by RBM oxidizing 5 mM succinate. In general, control RBM oxidizing succinate in the metabolic State 4 generate 6-8 times more H_2O_2 than RBM oxidizing glutamate or pyruvate (see Figures 7A and 7B). Figure 9A shows that with exception of antimycin A, addition of rotenone, myxothiazol (stigmatellin), or a combination of these inhibitors caused a significant inhibition of H_2O_2 generation. This suggests that most, but not all, of the succinate supported $O_2^{\cdot-}$ generation occurs on the Complex I reduced by the energy-dependent backward electron flow. This conclusion agrees with the earlier publications (42, 43). Addition of antimycin A caused a 3-fold increase in H_2O_2 generation that was abolished by a simultaneous addition of myxothiazol or stigmatellin (Fig. 9A). We have found no difference between myxothiazol and stigmatellin in their effects on succinate supported generation of H_2O_2 by RBM. Figure 9A shows that in the presence of myxothiazol + rotenone there was a substantial rate of H_2O_2 production (53 ± 10 pmol/min/mg protein) comparable with the State 4 rate of ROS generation with glutamate + malate (65 ± 5 pmol/min/mg protein). These are significantly higher rates for ROS generation reported recently for the rat heart mitochondria (42). However, the authors used incubation conditions which were not optimal for the heart mitochondria (sucrose medium, no Ca^{2+}, see ref. 31).

Figure 9B summarizes quantitatively the results of several experiments. Although systemic rotenone poisoning resulted in a reduced generation of ROS by RBM with succinate as a substrate (see Figures 7B and 9B) in the metabolic State 4, there was a significant increase in ROS generation by the Rot-RBM in the presence of myxothiazol and myxothiazol + rotenone (Figure 9B). In the presence of both myxothiazol and rotenone the electrons cannot go upstream or downstream the respiratory chain, and therefore the only source of ROS under these conditions may be the Complex II. After six days of rotenone infusion H_2O_2 generation becomes two times higher in the Rot-RBM (109 ± 6 pmol/min/mg protein) as compared to the control RBM (53 ± 10 pmol/min/mg protein). Thus the data

presented in Figures 9A and 9B argue that at least in RBM Complex II may also generate ROS that can be increased by a rotenone-induced damage to Complex II.

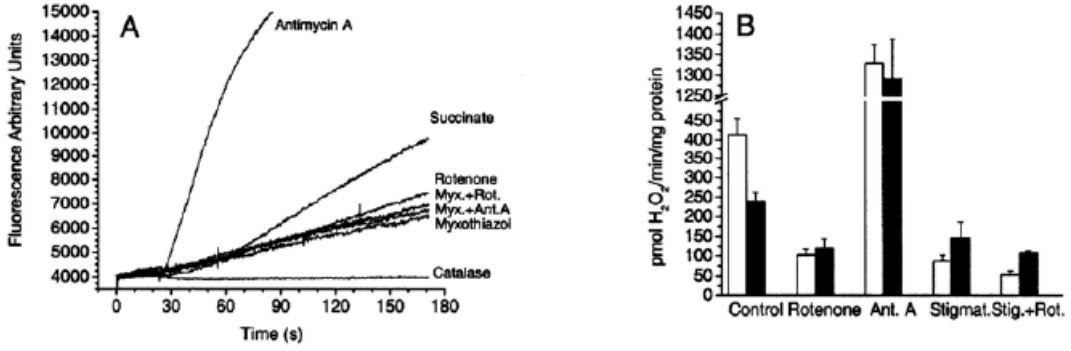

Figure 9. Effects of respiratory inhibitors on H_2O_2 generation by control RBM and Rot-RBM oxidizing succinate. Incubation conditions and additions as in Fig. 8. A. Responses of control RBM oxidizing succinate to additions of respiratory inhibitors; B. Generation of H_2O_2 by RBM from the control and rotenone-treated animals.

DISCUSSION

Previous studies have shown that the subcutaneous infusion of rotenone for 28 or 56 days reproduces many features of PD in rats including selective nigrostriatal dopaminergic degeneration (2, 17). In spite of numerous recent publications on rotenone toxicity *in vitro* (44, 45) and *in vivo* (1, 2, 18, 25, 26, 46, 47), the exact mechanisms of the specific rotenone-induced neurotoxicity remain obscure. Evidently during a long-term systemic rotenone infusion there is a complex interplay of the toxin's deleterious effects and defensive and adaptive mechanisms that in some neuronal cells fail to prevent the lethal outcome. It is known that toxic models of neurodegenerative diseases are subject to a large variability between various species as well as within one species (1, 26). In this study we exposed animals to rotenone infusion for six days in order to find the primary mechanisms of rotenone neurotoxicity that may be later disguised by adaptive reactions. It should be noted that unlike the long-term intoxication experiments, after six days of systemic rotenone infusion there was little variability between animals. For the first time we present data on the *in vivo* effects of rotenone on the three major mitochondrial functions, and define a cascade of early events that later may result in specific neurodegeneration.

Effects of the six days systemic rotenone infusion on mitochondrial respiration. Rotenone, when introduced *in vivo*, binds specifically to the mitochondrial Complex I (NADH:ubiquinone oxidoreductase) all over the brain, as revealed by [^{3}H]dihydrorotenone autoradiography (48), and we presume to Complex I in other tissues as well. With the rate of rotenone infusion by the Alzet osmotic pump at 3 mg/kg/24 h, it has been approximated that the concentration of "free" rotenone in brain should be about 20-30 nM (1). At this concentration rotenone had no inhibitory effect on the State 3 oxidation of glutamate + malate by isolated RBM, whereas with RLM it was inhibited by 50% (1). Although rotenone is a highly specific inhibitor of the mitochondrial Complex I, it also binds nonspecifically to proteins and hydrophobic compounds. Therefore, the actual concentration of rotenone in the tissues that is accessible to Complex I may be much lower than 20-30 nM. On the other hand, the amount of rotenone bound to Complex I can increase with time and thus gradually enhance inhibition of mitochondrial respiration. The steady-state degree of inhibition of RBM *in vivo* evidently depends on the rates of rotenone incoming from the Alzet pump and its removal by metabolism and excretion.

In control experiments we have found that isolation of mitochondria in the presence of 0.1% BSA completely removes rotenone bound to mitochondria (see Results). Therefore, the observed inhibitions of mitochondrial respiration with NAD-dependent substrates and succinate shown in Table I are associated with structural damages to Complex I and Complex II. After six days of rotenone infusion oxidations of the NAD-dependent substrates and succinate in metabolic states 3 and 3U were inhibited by 30-40%. However, we can presume that because *in vivo* rotenone is bound to Complex I, the inhibition of oxidation of the NAD-dependent substrates may be more than 40%. The unexpected fact that *in vivo* rotenone severely damages activity of Complex II argues that the inhibition was caused indirectly by a secondary mechanism that involves ROS because *in vitro* rotenone has no direct effect on activity of Complex II.

Effects of systemic rotenone toxicity on the Ca^{2+}-dependent Permeability Transition.

Although the control and Rot-RBM had the same State 4 membrane potential with glutamate + malate or succinate, our data show that in Rot-RBM diminished activities of Complex I or Complex II result in a decreased ability of the mitochondria to restore membrane potential during increased energy consumption. In agreement with this presumption, Rot-RBM have lower ability to sequester and retain CaPi even in the presence of ADP +

oligomycin. However, Rot-RBM protected by CsA + ADP had the same calcium retention capacity (CRC) as the control RBM.

Recently we have shown (33) that the Ca^{2+}-dependent mitochondrial permeability transition (mPT) depends on the two events: 1) energy-dependent sequestration of Ca^{2+} and Pi, and 2) interactions of Ca^{2+} and ADP with the pore-forming protein, which do not depend on mitochondrial energization. Evidently the reduced ability of Rot-RBM to maintain energization during Ca^{2+} and Pi sequestration was responsible for diminished CRC, while CsA-dependent mechanism of mPT was not affected. Because Rot-RBM underwent mPT at significantly lower Ca^{2+} loads than the control RBM, this would make neuronal cells (particularly glutamatergic neurons) more vulnerable to the Ca^{2+}-induced excitotoxic cell death.

Relatively small changes in the respiratory activity of the Rot-RLM and practically absence of the effects of systemic rotenone infusion on mPT may be explained by several mechanisms. First, hepatocytes have a powerful enzymatic machinery to metabolize rotenone. Second, liver has very high regenerative capacity and thus, the damaged cells would be eliminated and replaced by the "new" ones.

Effects of systemic rotenone toxicity on ROS generation by RBM.

Under normal conditions mitochondria in the actively functioning neuronal cells do not generate ROS because oxidative phosphorylation and other mitochondrial activities diminish the steady-state membrane potential and thus inhibit generation of ROS (38, 43). Therefore, investigations on the mitochondrial ROS generation under conditions of metabolic State 4 (which is a highly artificial situation) and the effects of various respiratory inhibitors reveal only a potential capacity of the given mitochondria to generate ROS under certain pathological conditions. The pathological situations that may increase generation of ROS by brain mitochondria include ischemia-reperfusion and hypoxia (reviewed in 49), Ca^{2+}-induced permeability transition (excitotoxicity) (43), drugs that inhibit respiratory activity (for example barbiturates), and poisoning with inhibitors of the respiratory chain, such as rotenone (50), MPT (51). Each of these pathological situations has evidently different impact on neuronal cells and mitochondria and different sequence of metabolic events that lead to a cell death.

In this paper we studied the effect of short-term systemic rotenone poisoning on mitochondrial functions. Recently It was shown that agricultural and household toxins may contribute to a rise of sporadic PD cases and probably other pathologies as well (23, 24). Thus, in order to find a corresponding prophylaxis measures and treatment methods it is important to understand the sequence of pathological events during systemic poisoning with mitochondrial toxins.

The data presented in this paper shows that the primary mechanism of systemic rotenone toxicity is an increase in generation of superoxide radical due to a partial inhibition and damage of Complex I. As we have shown earlier (1), the initial small doses of rotenone are too small to affect oxidative phosphorylation. Addition of rotenone *in vitro* to mitochondria increases generation of ROS at Complex I (see Fig. 7). Thus, it is not the primary inhibitory effect of rotenone on the electron transport activity of Complex I, but the resulting secondary mechanism – increased superoxide radical production is responsible for development of further structural and functional damages to mitochondria. We have previously discussed that rotenone toxicity results in a substantial loss of activity of Complex I and Complex II (see table I).

Table I. Effects of systemic rotenone infusion on oxidation by the rat brain and liver mitochondria of various substrates in different metabolic states.
Incubation conditions are described in Methods.

Rat Brain Mitochondria						
Succinate						**Glutamate**
RBM	**Rot-RBM**	**% Changes**	**RBM**	**Rot-RBM**		**% Changes**
State 4	120 ± 4	106 ± 2	-12 NS	54 ± 4	51 ± 4	-6 NS
State 3	498 ± 14	306 ± 19	-39 p<0.001	325 ± 17	242 ± 4	-26 <0.05
State 3U	523 ± 32	304 ± 17	-38 p<0.001	403 ± 25	305 ± 6	-29 p<0.05
Pyruvate						**α- Ketoglutoglutarate**
RBM	**Rot-RBM**	**% Changes**	**RBM**	**Rot-RBM**		**% Changes**
State 4	66 ± 6	49 ± 10	-26 NS	60 ± 5	50 ± 5	-17 NS
State 3	366 ± 17	218 ± 17	-40 p<0.05	292 ± 5	175 ± 6	-40 p<0.001

State 3U	511 ± 29	318 ± 26	-38 p<0.05	318 ± 12	213 ± 15	-33 p<0.01
Rat Liver Mitochondria						
Succinate						**Glutamate**
RLM	**Rot-RLM**	**% Changes**	**RLM**	**Rot-RLM**		**% Changes**
State 4	38 ± 4	39 ± 2	NS	25 ± 9	19 ± 2	NS
State 3	163 ± 16	139 ± 5	NS	127 ± 9	62 ± 2	-52 p<0.01
State 3U	267 ± 21	192 ± 4	NS	201 ± 14	87 ± 5	-57 p<0.01
Pyruvate						**α-Ketoglutoglutarate**
RLM	**Rot-RLM**	**% Changes**	**RLM**	**Rot-RLM**		**% Changes**
State 4	22 ± 2	22 ± 10	NS	26 ± 2	23 ± 2	NS
State 3	55 ± 2	38 ± 3	-31 p<0.05	58 ± 3	24 ± 2	-59 p<0.05
State 3U	63 ± 2	48 ± 3	NS	52 ± 3	42 ± 3	NS

Mechanism of damages to Complex I and Complex II. The most likely mechanism of the decreased activities of the two complexes is a damage of the 4Fe-4S clusters in these complexes caused by superoxide radical ($O_2^{\cdot-}$) and/or peroxynitrite ($ONOO^-$). Previous works revealed that enzymes containing 4Fe-4S clusters are particularly vulnerable to damage by these two radicals (52-54). Bashkatova et al (25) have shown that after ten days of chronic rotenone intoxication there was no increase in the levels of nitric oxide (NO), or lipid-peroxidation like products that would result from increased generation of $ONOO^-$. Thus, it is plausible that after the short-term poisoning with rotenone the inhibitions of Complexes I and II were primarily associated with increased generation of $O_2^{\cdot-}$. Even if $ONOO^-$ does participate in the damage to the respiratory enzymes its generation depends on increased levels of both NO and $O_2^{\cdot-}$.

The most evident proof of a particular vulnerability of the 4Fe-4S clusters was obtained in experiments with aconitase and some other enzymes of aconitase family (52-54). Complex II has one and Complex I has six 4Fe-4S clusters (see Figure 10).

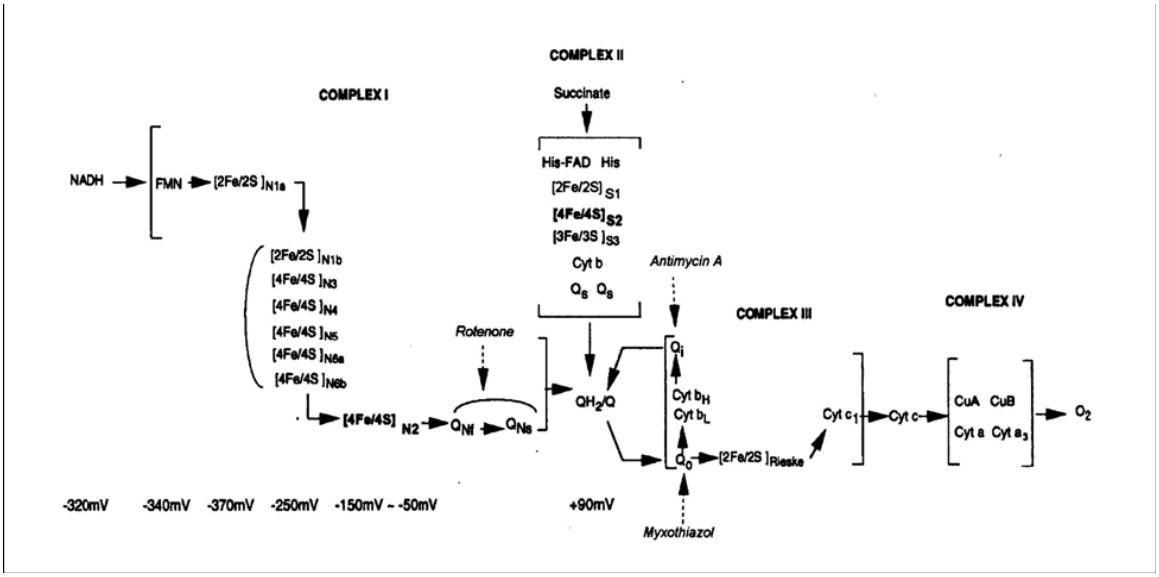

Figure 10. Respiratory components in mammalian mitochondria. The figure was adapted from (42).

It is thus logical to suggest that these structures are also highly sensitive to the damaging effects of $O_2^{\cdot-}$ and $ONOO^-$. Because Complex I has more 4Fe-4S clusters than Complex II, one would expect that chronic systemic rotenone intoxication would cause more damage to Complex I than Complex II. However, we have found that both Complex I and Complex II were damaged to the same degree. The explanation of this "controversy" arises from recent work by Ohnishi et al (42). These authors suggested that cluster N2 and bound semiquinones play key roles in the function of complex I, such as electron transfer, proton transport, and superoxide generation. Other five 4Fe-4S

clusters of Complex I are protected from reacting with oxygen (54). The only exception may be cluster N2 (42). It has been hypothesized that this cluster may serve as the coupling site between electron transfer and proton transport in complex I (56). This requires that the region of cluster N2 and protein-bound ubisemiquinones must be accessible to H^+ and water. Hence, this region is also accessible to oxygen and the possibility of reducing oxygen to superoxide would also occur (42).

Complex II as a site of ROS production. When discussing generation of ROS by mitochondria, only Complex I and Complex III are usually considered as the major sites for production of superoxide radical by normal *in situ* and isolated mitochondria. After years of controversy recent X-ray studies have shown that the [4Fe-4S] cluster is part of a linear electron transport chain located between FAD cofactor and the quinone or *b* heme (reviewed in 57). Thus, the [4Fe-4S] cluster of Complex II can also be a target for the damaging effects of $O_2^{\cdot-}$ and $ONOO^-$ radicals. There are known human diseases associated with mutations of genes for Complex II and interestingly many of these mutations cause various tumors (57).

Studies of bacterial or yeast mitochondria (reviewed in 57) have shown that Complex II (succinate:quinone oxidoreductase) is capable of generating only $O_2^{\cdot-}$ which occur presumably at the FAD cofactor (58). In our experiments we used a highly sensitive fluorometer to find that in the presence of myxothiazol or myxothiazol + rotenone RBM oxidizing succinate do generate ROS (measured as H_2O_2) at a rate (53 ± 10 pmol/min/mg protein) comparable with that in the presence of Complex I substrates (65.5 ± 8 pmol/min/mg protein). Although systemic treatment of rats with rotenone caused a 42% decrease of ROS generation on Complex I due to a succinate-driven backward electron flow (see Fig. 7B and Fig. 9B), generation of ROS on Complex II in the presence of rotenone + myxothiazol increased two times (109 ± 5 pmol/min/mg protein, see Fig. 9B) after six days, and three times (156 ± 15 pmol/min/mg protein) after four weeks of rotenone intoxication.

We presume that an important consequence of the damaging of [4Fe-4S] clusters is a shift of the major sites of SO generation. Figure 10 shows the sequence of electron transport chain components in mammalian mitochondria. The tentative damaged [4Fe-4S] clusters in Complex I and Complex II are shown in bold. One can see that because of the imposed limit on the electron transport by the damages to [4Fe-4S] clusters in both complexes, there must be a higher reduction of components located before the damage. As a result, flavin components of the Complex I and Complex II will be in a more reduced state and thus may produce more $O_2^{\cdot-}$ (58). We have already mentioned that in active mitochondria under normal conditions membrane potential is significantly lower that that observed in the Metabolic State 4. Therefore, normal mitochondria generate very little ROS and it is strongly dependent on the functional state of the mitochondria. However, in the rotenone-treated animals the limits imposed on electron transport by the damages to Complex I and II make generation of ROS not dependent any more on the functional state of the mitochondria. Evidently, even a slow but constant generation of mitochondrial ROS may be very harmful for the neuronal cells, particularly when glial generation of NO increases.

Our data show that a relatively brief (six days) intoxication with rotenone does not result in a significant amount of damage of lipid membranes. Our data support the idea that inactivation of Complex I and Complex II was mediated by an increase in formation of $O_2^{\cdot-}$ and $ONOO^-$ because they are chemically active and can reach their specific targets, one of which are 4Fe-4S clusters in various enzymes.

We show that systemic intoxication of animals with a highly specific inhibitor of Complex I also results in a damage of Complex II. This fact indicates that the concepts that associate damages of Complex I with Parkinson's disease, and damages of Complex II with Huntington's disease are at least too simplistic. Our data show that even a brief systemic exposure of an animal to rotenone caused multiple mitochondrial dysfunctions, which are interconnected and each of them may probably cause cell's demise by different death pathway.

Altogether our data shows that in order to understand the role of mitochondria in the pathogenesis of NDD various mitochondrial functions have to be studied. The multiple natures of mitochondrial dysfunctions have to be considered when designing methods of cure or prophylaxis of NDD.

FOOTNOTES

The authors thank Dr. John Watts for valuable discussion, and Kim Wilson for her help in editing the text of the paper. The authors gratefully acknowledge support from the Parkinson's Disease Society of America (JTG)

REFERENCES

1. Betarbet, R., Sherer, T.B., MacKenzie, G., Garcia-Osuna, M., Panov, A.V., and Greenamyre, J.T. (2000) *Nat. Neurosci.* **3**, 1301-1306

2. Betarbet, R., Sherer, T.B., and Greenamyre, J.T. (2002) *Bioessays*. **24**, 308-318

3. Panov, A.V., C-A. Gutekunst, B. R. Leavitt, M. R. Hayden, Burke, J.R., Strittmatter, W.J., and J.T. Greenamyre. (2002) *Nature Neuroscience*. **5**, 731-736

4. Cluskey, S., and Ramsden, D.B. (2001) *Mol. Pathol*. **54**, 386-392

5. Calabrese, V., Lodi, R., Tonon, C., D'Agata, V., Sapienza, M., Scapagnini, G., A. Mangiameli, A., Pennisi, G., A. Stella, A.M., and D. A. Butterfield (2005). *J. Neurol. Sci.* **233,** 145-162

6. Beal, M.F. (1996) *Curr. Opin. Neurobiol*. **6**, 661-666
7. Fiskum, G., Starkov, A., Polster, B.M., and Chinopoulos, C. (2003) Ann. NY Acad. Sci. **991**, 111-119
8. Beal, M.F. (1998) *Biochim. Biophys. Acta*. **1366**, 211-223
9. Schober, A. (2004) *Cell Tiss. Res*.**318**, 215-224
10. Beal, M.F. (1996)] *Curr. Opin. Neurobiol*. 6, 661-666
11. Beal, M.F. (2003) *Ann. N.Y. Acad. Sci*. **991**, 120-131
12. Beal, M.F. (2001) *Nat. Rev. Neurosci*. **2**, 325-334
13. Greenamyre, J.T., Sherer, T.B., Betarbet, R., and Panov, A.V. (2001) *IUBMB Life*. **52**, 135-141
14. Emerit, J., Edeas, M., and Bricaire, F. (2004) *Biomed. Pharmacother*. **58**, 39-46
15. Echaniz-Laguna, A., Zol,l J., Ribera, F., Tranchant, C., Earter, J-M., Lonsdorfer, J., and Lampert, E. (2002) *Ann Neurol*. **52**, 623-627
16. Schober, A. (2004) *Cell Tiss. Res*. **318**, 215-224
17. Sherer, T.B., Kim, J-H., Betarbet, R., and Greenamyre, J.T. (2003) *Exp. Neurol*. **179**, 9-16
18. Hoglinger, G.U., Feger, J., Prigent, A., Michel, P.P., Parain, K., Champy, P., Ruberg, M., Oertel, W.H., and Hirsh, E.C. (2003) *J. Neurochem*. **84**, 491-502
19. Uversky, V.N. (2004) *Cell Tissue Res*.**318**, 225-241
20. Borlongan, C.V., Nishino, H., and Sanberg, P.R. (1997) *Neurosci. Res*. **28**, 185-189
21. Brouillet, E., Conde, F., Beal, M.F., and Hantraye, P. (1999) *Prog. Neurobiol*. **59**, 427-468
22. Greene, J.G., and Greenamyre, J.T. (1995) *J. Neurochem*. **64**, 2332-2338
23. Priyadarshi, A., Khuder, S.A., Schaub, E.A., and Priyadarshi, S.S. (2001) *Environ Res*. **86**, 122-127
24. Vanacore, N., Nappo, A., Gentile, M., Brustolin, A., Palange, S., Liberati, A., Di Rezze1, S., Caldora1, G., Gasparini1, M., Benedetti, F., Bonifati1, V., Forastiere, F., Quercia, A., and Meco1, G. (2002) *Neurol. Sci*. **23**, Suppl 2, S119-S120
25. Bashkatova, V., M. Alam, M.m, Vanin, A., and Schmidt, W.J. (2004) *Experim. Neurol*. **186**, 235-241

26. Lapointe, N., St-Hilaire, M., Martinolli, M-G., Blanchet, J, Gould, P., Rouillard, C., and Cicchetti, F. (2004) *FASEB J*. **18**, 717-719
27. Jenner, P. (2003) Ann. Neurol. **53**, Suppl. 3, S26-S38
28. Panov, A., and Scarpa, A. (1996) *Biochem*. (USA), **35**, 12849-12856
29. Lee, C-P., and Ernster, L. (1967) *Methods in Enzymology*, Estabrook, R.W. and Pullman, M.E., eds., pp. 543-548, AP., NY – London
30. Sims, N.R. (1990) *J. Neurochem*. **55**, 698-707
31. Panov, A.V., and Scaduto, R.C., Jr. (1996) *Am. J. Physiol. Heart Circ. Physiol.*, **270**, H1398-H1406
32. LaNoue K.F., Jeffries F.M.H., Radda G.K.. Kinetic control of mitochondrial ATP synthesis. Biochemistry, 25 (1986) 25, 7667-7675
33. Panov, A., Andreeva, L., and Greenamyre, J.T. (2004) *Arch. Biochem. Biophys*. **424**, 44-52
34. Dikalov, S.I., Dikalova, A.E., and Mason, R.P. (2002) *Arch. Biochem. Biophys*. **402**, 218-226
35. Koopman, W. J., Verkaart, S., Visch, H.J., van der Westhuizen, F.H., Murphy, M.P., van den Heuvel, L.W., Smeitink, J.A., and Willems, P.H. (2005). *Am. J. Physiol. Cell Physiol*. **288**, C1440-1450
36. Brookes, P.S. (2005) *Free Rad. Biol. Med*. **38**, 12-23
37. Reynolds, I.J. (1999) *Ann. NY Acad. Sci*. **893**, 33-41
38. Chalmers, S., and Nicholls, D.G. (2003) *J. Biol. Chem*. **278**, 19062-19070
39. Andreeva, L., and Crompton, M. (1994) *Eur. J. Biochem*. **221**, 261-268
40. Cadenas, E., Boveris, A., Ragan, C.I., and Stoppani, A.O.M. (1977) *Arch. Biochem. Biophys*. **180**, 248-257
41. Santos, M.S., Santos, D.L., Palmeira, C.M.N., Seica, R., Moreno, A.J., and Oliveira, C.R. (2001) *Diabetes Metab. Res. Rev*. **17**, 223-230
42. Ohnishi, S.T., Ohnishi, O., Muranaka, S., Fujita, H., Kimura, H., Uemura, K., Yoshida, K-i., and Utsumi, K. (2005) *J. Bioenerg. Biomembr*. **37**, 1-15
43. Votyakova, T.V., and Reynolds, I.J. (2005) *J. Neurochem*. **93**, 526-537
44. Sherer, T.B., Betarbet, R., Stout, A.K., Lund, S., Baptista, M., Panov, A.V., Cookson, M.R., and Greenamyre, J.T. (2002) *J Neurosci*. **22**, 7006-7015
45. Isenberg, J.S., and Klaunig, J.E. (2000) *Toxicol. Sci*. **53**, 340-351
46. Sherer, T.B., Kim, J-H., Betarbet, R., and Greenamyre, J.T. (2003) *Experim. Neurol*. **179**, 9-16
47. Sherer, T.B., Betarbet, R., Kim, J.H., and Greenamyre, J.T. (2003) *Ann. Neurol*. **341**, 87-90
48. Greenamyre, J.T., Higgins, D.S., and Eller, R.V. (1992) *J. Neurochem*. **59**, 746-749
49. Chakraborti, T., Das, S., Mondal, M., Roychoudhury, S., and Chakraborti, S. (1999). Cell Signal. **11**, 77-85.
50. Sherer, T.B., Betarbet, R., Testa, C.M., Seo, B.B., Richardson, J.R., Kim, J.H., Miller, G.W., Yagi, T., Matsuno-Yagi, A., and Greenamyre, J.T. (2003) *J Neurosci*. **23**,10756-10764
51. Cassarino, D.S., Fall, C.P., Swerdlow, R.H., Smith, T.S., Halvorsen, E.M., Miller, S.W., Parks, J.P., Parker, W.D. Jr., and Bennett, J.P., Jr. (1997) *Biochim. Biophys. Acta*. **1362**, 77-86
52. Fridovich, I. (1995) *Annu. Rev. Biochem.* **64,** 97-112
53. Flint, D.H., Tuminello, J.F., and M. Emptage, M.H. (1993). *J. Biol. Chem.* **268**, 22369-22376
54. Bouton, C., Raveau, M. and Drapier, J.C. (1996). *J. Biol. Chem.* **271**, 2300-2306
55. Vinogradov, A.D. (1998) *Biochim. Biophys. Acta*, 1364, 169-185
56. Ingledew, W.J., and Ohnishi, T. (1980) *Biochem. J*. 186, 111–117
57. Cecchini, G. (2003) *Ann. Rev. Biochem*. **72**, 77-109
58. Massey, V. (1994) *J. Biol. Chem*. **269**, 22459-22462